

RESEARCH

Open Access



Improved energy efficiency in microbial fuel cells by bioethanol and electricity co-generation

Rong Xie, Shuang Wang, Kai Wang, Meng Wang, Biqiang Chen, Zheng Wang and Tianwei Tan*

Abstract

Background: Microbial electricity production has received considerable attention from researchers due to its environmental friendliness and low price. The increase in the number of intracellular electrons in a microbial fuel cell (MFC) helps to improve the MFC performance.

Results: In this study, we accumulated excess electrons intracellularly by knocking out the gene related to intracellular electron consumption in *Saccharomyces cerevisiae*, and the elevated intracellular electron pool positively influenced the performances of MFCs in terms of electricity production, while helping to increase ethanol production and achieve ethanol and electricity co-production, which in turn improved the utilization of substrates. The final knockout strain reached a maximum ethanol yield of 7.71 g/L and a maximum power density of 240 mW/m² in the MFC, which was 12 times higher than that of the control bacteria, with a 17.3% increase in energy utilization.

Conclusions: The knockdown of intracellular electron-consuming genes reported here allowed the accumulation of excess electrons in cells, and the elevated intracellular electron pool positively influenced the electrical production performance of the MFC. Furthermore, by knocking out the intracellular metabolic pathway, the yield of ethanol could be increased, and co-production of ethanol and electricity could be achieved. Thus, the MFC improved the utilization of the substrate.

Keywords: Microbial fuel cells, *Saccharomyces cerevisiae*, Ethanol, Electricity

Background

The use of fossil energy leads not only to global climate change, but also to an increase in energy shortages due to the non-renewable nature of fossil energy [1]. Renewable energy use can help solve the current problems of energy shortages and inadequate power supplies, as well as achieve sustainable development, efficient use, and resource conservation of energy [2]. As one of the most promising biofuels to replace fossil fuels, bioethanol has the advantage of being widely used and derived from renewable products (e.g., biomass such as straw) [3].

Microorganisms can produce ethanol from raw materials such as molasses and cellulose under the action of fermentation. As a microorganism suitable for industrial production, brewer's yeast has a long history of fermenting and producing ethanol, and it is easy to cultivate, fast growing and metabolism, simple and cheap, safe and highly tolerant of ethanol [4]. Under anaerobic conditions, 1 mol of glucose will produce 2 mol of pyruvate. Pyruvate will be catalyzed by pyruvate decarboxylase and is further oxidized to 2 mol acetaldehyde and 2 mol carbon dioxide is produced. Next, 2 mol of acetaldehyde is passed through ethanol dehydrogenase to produce 2 mol of ethanol. Since ethanol dehydrogenase is an NADH-dependent enzyme, the intracellular accumulation of NADH is able to increase ethanol production to some extent [5, 6]. In addition, the fermentation of organic matter by brewer's yeast to produce ethanol is

*Correspondence: twtan@mail.buct.edu.cn

National Energy R&D Center for Biorefinery, Beijing Key Lab of Bioprocess, College of Life Science and Technology, Beijing University of Chemical Technology, No. 15 North 3rd Ring Rd East, Beijing 100029, People's Republic of China



© The Author(s) 2022. **Open Access** This article is licensed under a Creative Commons Attribution 4.0 International License, which permits use, sharing, adaptation, distribution and reproduction in any medium or format, as long as you give appropriate credit to the original author(s) and the source, provide a link to the Creative Commons licence, and indicate if changes were made. The images or other third party material in this article are included in the article's Creative Commons licence, unless indicated otherwise in a credit line to the material. If material is not included in the article's Creative Commons licence and your intended use is not permitted by statutory regulation or exceeds the permitted use, you will need to obtain permission directly from the copyright holder. To view a copy of this licence, visit <http://creativecommons.org/licenses/by/4.0/>. The Creative Commons Public Domain Dedication waiver (<http://creativecommons.org/publicdomain/zero/1.0/>) applies to the data made available in this article, unless otherwise stated in a credit line to the data.

accompanied by the oxidation of large amounts of NADH to NAD⁺.

The intracellular reduced coenzyme NADH or NADPH can be collected in the form of electrons for power generation. Microbial devices that use organic or inorganic feedstocks to generate electricity are often called microbial fuel cells (MFCs). In microbial fuel cells, microorganisms transfer electrons to solid electrodes. Anode microbial fuel cells can be divided into two categories based on microbial utilization. Fuel cells in the first category utilize a single compound, such as glucose [7, 8], xylose [9], cellulose [10], or acetate [11], and use a single strain of bacteria as the inoculum source for MFCs. Fuel cells in the second category usually use waste with a complex composition, such as domestic sewage [12], industrial wastewater [13], medical wastewater [14], and other types of wastewater (e.g., straw hydrolysate, human excreta) [15–18], and use colonies in the sludge as a source of inoculum for MFC. Microorganisms in the anode transfer electrons to the electrode, while microorganisms from the cathode can catalyze oxygen reduction reactions instead of inorganic catalysts, receiving electrons [19, 20]. Some microorganisms are attached to the electrode, and intracellular electrons can be transferred directly to the electrode, i.e., direct electron transfer (DET), while microorganisms free in the medium need an electron transfer medium to achieve electron transfer [21, 22]. In microbial fuel cells, the electron transfer efficiency is improved by adding redox mediators, genetic engineering methods to modify microorganisms, using materials with better electrical conductivity as electrodes, and so on. For example, Lithuania et al. summarized the biocompatibility of conducting polymers, which are commonly used in biofuel cells to improve the electron transfer efficiency [23, 24]. In addition, two-dimensional materials such as MXenes are often used in the design of biosensors and biofuel cells to improve the electron transfer efficiency [25].

Due to the partial energy consumption of *Saccharomyces cerevisiae* during the fermentation for ethanol production, the energy utilization is reduced. When microbial fuel cells use substrates to generate electricity, the substrates have less application in the production of the product. Thus, by culturing *Saccharomyces cerevisiae* in a microbial fuel cell anode chamber, on the one hand, the microorganisms can use the substrate for fermentation to produce ethanol. On the other hand, electrons

generated from the NADH/NAD⁺, NADPH/NADP⁺ redox cycle can be extracted for power generation by using MFC technology. Thus, by harvesting some of the energy that would otherwise be lost during the fermentation process in the form of electrical energy, the utilization of the substrate is improved.

In this work, we constructed a dual-chamber microbial fuel cell in which modified *Saccharomyces cerevisiae* in the anode chamber utilized glucose for ethanol production and transferred excess intracellular electrons—in the form of the electron carrier NAD(P)H—to the anode electrode via an electron transfer mediator, with the cathode K₃[Fe(CN)₆] acting as the electron acceptor. The regulation of intracellular metabolic pathways in *Saccharomyces cerevisiae* mainly targets two modules—the pyruvate metabolism and the citric acid cycle—by knocking down 12 genes that consume NAD(P)H intracellularly and regulating the intracellular NADH/NAD⁺ and NADPH/NADP⁺ ratios (Fig. 1), thus affecting the intracellular electron content and the extracellular electron transfer (EET) rate.

Results

Performance of ethanol and electricity co-production by knockout strains of lactate dehydrogenase in pyruvate metabolism

In *Saccharomyces cerevisiae* cells, lactate synthesis is a reduction pathway catalyzed by lactate dehydrogenase in the pyruvate metabolism, and this reduction process is accompanied by the oxidation of NADH to NAD⁺ (i.e., electron-consuming pathway). Therefore, knocking out the gene associated with lactate dehydrogenase enables the accumulation of electrons in the cell, which are then directed to the anode via an electron transfer mediator. Since the process of ethanol fermentation is accompanied by a large amount of NADH consumption [26], the NADH accumulated after knocking out the gene related to lactate dehydrogenase is also conducive to increase the ethanol production at the same time. To verify the performance of the modified strain for ethanol and electricity co-production using glucose in MFCs, the cell growth, ethanol yield, and electricity production performance were studied in an open circuit and an external circuit.

The growth curves of the strains (Additional file 1: Fig. S1) show that the OD of most of the knockout strains did not differ much from the growth of the original bacteria, so knocking out the lactate dehydrogenase-related

(See figure on next page.)

Fig. 1 **a** Schematic diagram of yeast microbial fuel cell. **b** Regulation of the *Saccharomyces cerevisiae* metabolic pathway to accumulate excess electrons in the yeast cell. Knockdown of genes associated with NAD(P)H depletion in yeast cells (marked in red), specifically lactate dehydrogenase genes *dld1*, *dld2*, *dld3* in the pyruvate metabolism and genes associated with depletion of reduced coenzymes in the citric acid cycle including mitochondrial malic enzyme *mae*, malate dehydrogenase *mdh1*, *mdh2*, *mdh3*, NADP-specific isocitrate dehydrogenases *idp1*, *idp2*, *idp3*, old yellow enzyme *oye2*, *oye3*.

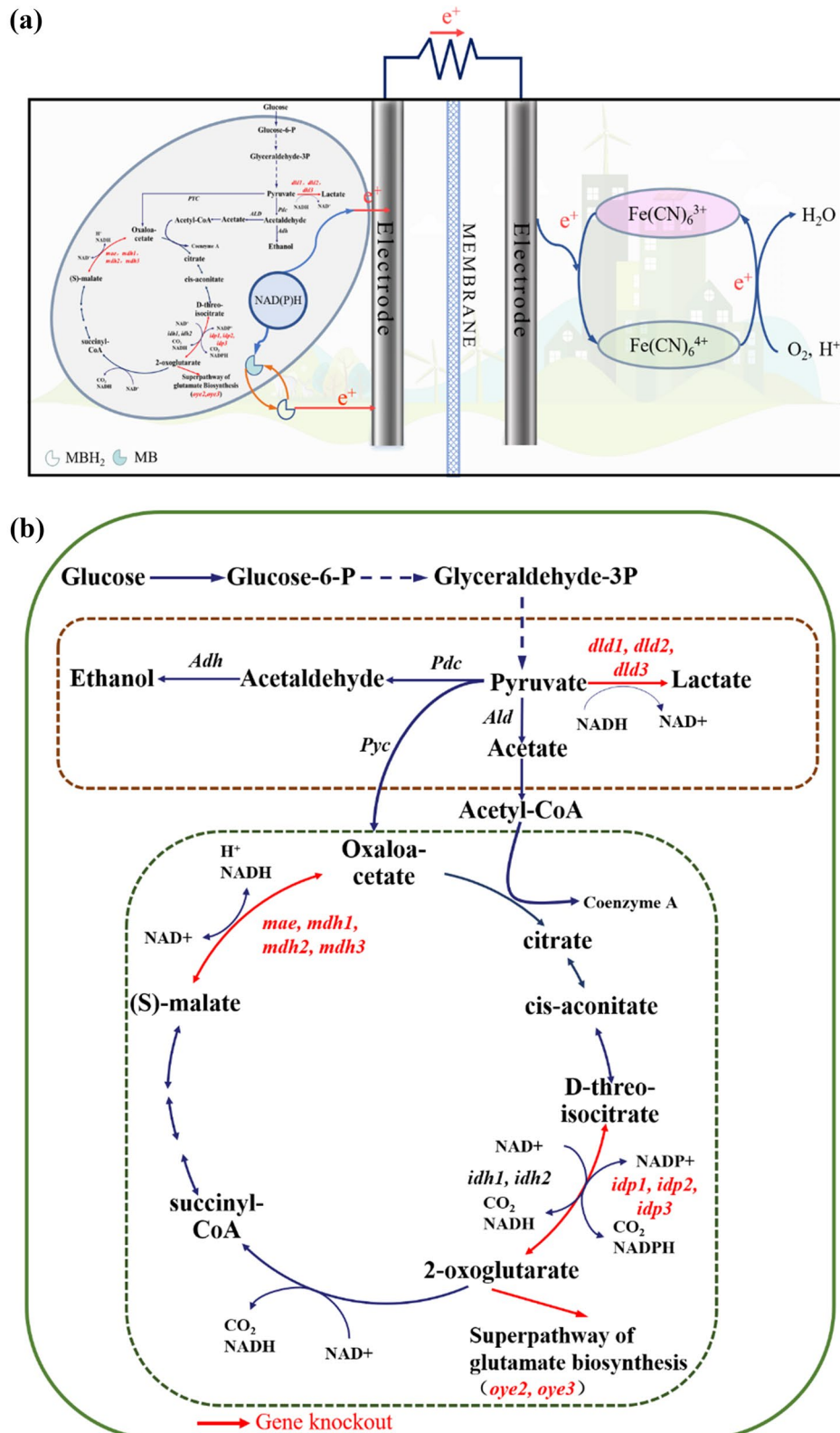


Fig. 1 (See legend on previous page.)

genes in the pyruvate metabolism had little effect on the microbial growth. The knockout strains were examined for glucose consumption and ethanol production during the fermentation of ethanol using glucose in the open circuit and the external circuit, respectively. The

results showed that the highest yields of ethanol production from glucose fermentation by the $\Delta dld1$, $\Delta dld2$, $\Delta dld3$, $\Delta dld12$, $\Delta dld13$, and $\Delta dld23$ strains reached 6.24, 7.01, 5.72, 7.55, 6.72, and 6.18 g/L, respectively (Fig. 2a, b). The $\Delta dld123$ strain with all the lactate dehydrogenase

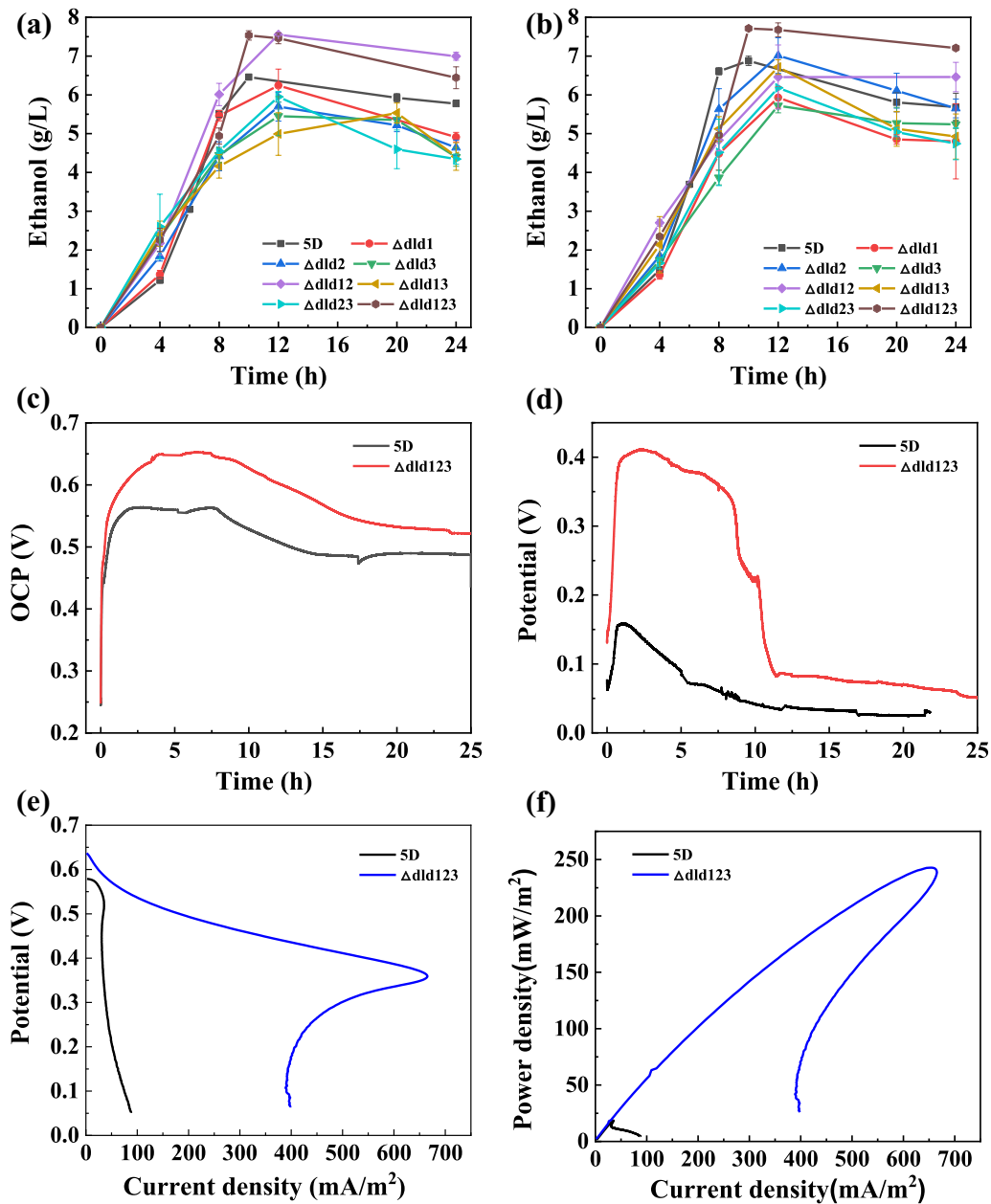


Fig. 2 Ethanol and electricity co-production performances of knockout strains of lactate dehydrogenase. **a** Ethanol production yields of *5D*, $\Delta dld1$, $\Delta dld2$, $\Delta dld3$, $\Delta dld12$, $\Delta dld13$, $\Delta dld23$, and $\Delta dld123$ knockout strains using glucose when run in the microbial fuel cell (MFC) for 24 h in an open circuit. **b** Ethanol production yields *5D* and seven knockout strains using glucose when run in the MFC for 24 h in an external circuit. **c** Open-circuit potential (OCP) of original *5D* strain and $\Delta dld123$ strain running in the MFC for 24 h. **d** External-circuit potential of original *5D* strain and $\Delta dld123$ strain operating in the MFC for 24 h with a 1000 Ω resistor connected externally in the MFC. **e** Linear scan voltammetry curves of the original *5D* strain and the $\Delta dld123$ strain in the MFC at a sweep speed of 2 mV/s. **f** Power density curves of the original *5D* strain and the $\Delta dld123$ strain in the MFC at a sweep speed of 2 mV/s. The MFC was run at 35 °C and 500 rpm. Values are shown as the mean \pm s.d. ($n=3$)

genes knocked out had the highest ethanol yield of 7.71 g/L and the highest yield of 38.6% of all the knock-out strains with external linkage resistance. The knockout strain consumed glucose at a similar rate to that of the original *5D* strain, with glucose being consumed at about 10 h. The specific values of the glucose consumption rate in the open circuit and the external circuit are shown in Additional file 1: Fig. S2. This indicates that knocking out all the relevant genes of lactate dehydrogenase does not affect ethanol production. This may be ascribed that knocking out lactate dehydrogenase leads to a greater flow of carbon sources into ethanol, resulting in a slight increase in ethanol production. However, it could also be due to the intracellular accumulation of more NADH, which increases the intracellular reducing power, resulting in an increase in ethanol production [26].

The MFC electrical production performance is shown in Fig. 2. The open-circuit potential of both the original and modified strains reached the highest value within the first 4 h. The highest open-circuit potential of the *5D* original bacteria reached 0.56 V. Figure 2c shows that the open-circuit potential of $\Delta dld123$ strain was significantly increased compared with that of the original bacteria, reaching 0.65 V, which was 16% higher than that of the original bacteria. The highest open-circuit potentials of $\Delta dld1$, $\Delta dld2$, $\Delta dld3$, $\Delta dld12$, $\Delta dld13$, and $\Delta dld23$ strains were 0.6, 0.586, 0.593, 0.584, 0.623, and 0.582 V, respectively (Additional file 1: Fig. S3), higher than the original open-circuit potential but lower than that of the $\Delta dld123$ strain. The MFC showed a rapid decrease in the open-circuit potential for all strains after 10 h of operation, and the external circuit showed the same trend as the open circuit. The *5D* original strain had the highest external-circuit potential of 0.16 V, and among the other modified strains, the $\Delta dld123$ strain had the highest external-circuit potential of 0.411 V, which was 157% greater than that of the original strain. However, the external circuit decayed more rapidly to only about 0.04 V at about 10 h. The reason for the decay of the open-circuit potential and the external-circuit potential may be that after the consumption of the substrate glucose, the electron supply is insufficient, resulting in the decay of the open-circuit potential and a corresponding decay of the external circuit. However, the decay of the external circuit is more rapid due to the consumption of electrons [27–29]. The greater improvement in the electricity production performance of the modified strain compared to that of the original *5D* strain may be due to the intracellular accumulation of more NADH after knocking out the gene related to lactate dehydrogenase. These accumulated electrons are in turn transferred to the electrode through the electron transfer medium methylene blue (MB), resulting in an increase in the open-circuit potential

and external-circuit potential [26]. The performance of the microbial fuel cell was evaluated by linear scanning voltammetry at the open-circuit potential, and the results are shown in Fig. 2e, f. The results showed that the $\Delta dld123$ strain had the highest power density, and the other knockout strains had power densities between 45 and 55 mW/m², which were 2–3 times greater than that of the original bacteria. The highest power density of the $\Delta dld123$ strain reached 240 mW/m², which was 12 times greater than that of the original bacteria. The power density data for the remaining strains are shown in Additional file 1: Fig. S4. The large increase in the power density may be attributed to the accumulation of more electrons in the cell, which increases EET rate, resulting in a decrease in the internal resistance of the MFC [30], an increase in the external-circuit potential, and thus, an increase in the power density [31].

During the analysis of the power density curve, we observed the power overshoot phenomenon (Fig. 2e). The reasons for this phenomenon may be that by anode limitation, such as electron depletion phenomenon due to proton accumulation and substrate limitation, poor enrichment of biofilm, etc. [32, 33]. However, the power overshoot appears to be only a temporary system overload, as we observed that the microorganisms were able to overcome this overload during the ongoing polarization scan. Ieropoulos et al. proposed that during recovery, the electron/ion supply/demand balance is restored and the power profile exits the overload mode as the current starts to increase [34]. The recovery highlights the robustness of the microbial culture and its ability to adjust to dynamic and even hostile conditions, which can be attributed to the continuous replenishment of the depleted substrate [35].

Performance of ethanol and electricity co-production by knockout strains of genes related to partial depletion of reduced coenzymes in the tricarboxylic acid cycle

After glucose is oxidized to pyruvate through the process of glycolysis, pyruvate is further oxidized to organic acids in the tricarboxylic acid cycle (TCA cycle). Since some pathways accumulate electrons in the TCA cycle [36], knockdown of some genes related to the consumption of reduced coenzymes in the TCA cycle (as marked by the TCA module in Fig. 1) is considered to result in the accumulation of electrons and improve the electricity production performance. The specific knockdown genes are shown in Table 1.

Knockout strains of genes associated with NAD(P)H consumption in the TCA cycle were similarly investigated for the ethanol electricity co-production performances of the knockout strains in terms of microbial growth, ethanol yield, and electricity production performance. The

Table 1 Selected genes associated with the depletion of reduced coenzymes in the TCA cycle

Gene name	Pathway	Reaction	Dependency
<i>mae</i>	TCA cycle	(S)-malate + NAD ⁺ → CO ₂ + pyruvate + NADH	NAD-dependent enzyme
<i>idp1, idp2, idp3</i>	Glutamate biosynthesis	D-threo-isocitrate + NADP ⁺ ↔ 2-oxoglutarate + CO ₂ + NADPH (reversible)	NADP-dependent enzyme
<i>mdh1, mdh2, mdh3</i>	TCA cycle	(S)-malate + NAD ⁺ ↔ oxaloacetate + NADH + H ⁺ (reversible)	NAD-dependent enzyme
<i>oye2, oye3</i>	Sterol metabolism, citronellol synthesis	Oxidized electron acceptor + NADPH + H ⁺ ↔ reduced electron acceptor + NADP ⁺ (reversible)	NADPH-dependent enzyme

glucose consumption and ethanol production amounts of the knockout strains in the open circuit and the external circuit were examined separately. The ethanol production amounts of the knockout strains using glucose fermentation are shown in Fig. 3a, b. Aside from the highest ethanol production of 7.33 g/L for the $\Delta mdh1$ knockout strain, the ethanol production amounts of all the knockout strains decreased compared to that of the original *SD* strain. The glucose consumption rates of the knockout strains were lower, and there was glucose remaining in the anode electrolyte at 10 h (Additional file 1: Fig. S6). We observed from the strain growth curves (Additional file 1: Fig. S5) that most of the knockout strains had lower OD values than the original bacteria. The analysis of the reduction in ethanol yield after knockdown of some genes related to the depletion of reduced coenzymes in the TCA cycle may have occurred because the TCA cycle both provides energy for microbial life activities and is involved in the final metabolic pathway of the microorganism [37]. Therefore, the knockdown of the relevant genes in the TCA cycle will have an impact on microbial growth and nutrient metabolism, ultimately leading to a reduction in growth and ethanol yield.

The open-circuit and external-circuit potentials of the original bacteria and knockout strains are shown in Fig. 3c, d, respectively. The open-circuit potentials of the $\Delta oye3$ and $\Delta idp1$ knockout strains increased more significantly than those of other knockout strains, reaching 0.631 and 0.615 V, respectively, corresponding to increases of 12.7% and 9.8% compared with that of the original bacteria. A more significant increase in the external-circuit potential was observed for the $\Delta idp2$ and $\Delta oye3$ knockout strains, which reached 0.274 and 0.409 V, respectively. The performance of the microbial fuel cell was evaluated by linear voltammetry scanning, and the results showed that the highest power density of the $\Delta oye3$ strain reached 103.6 mW/m², which was 5.6 times higher than that of the original bacteria. Most of the other knockout strains had power densities between 50 and 65 mW/m², which were about three times higher than that of the original bacteria (Fig. 3e, f). Compared to the original *SD* strain, the strains that knocked out some of the genes related to the consumption of reduced

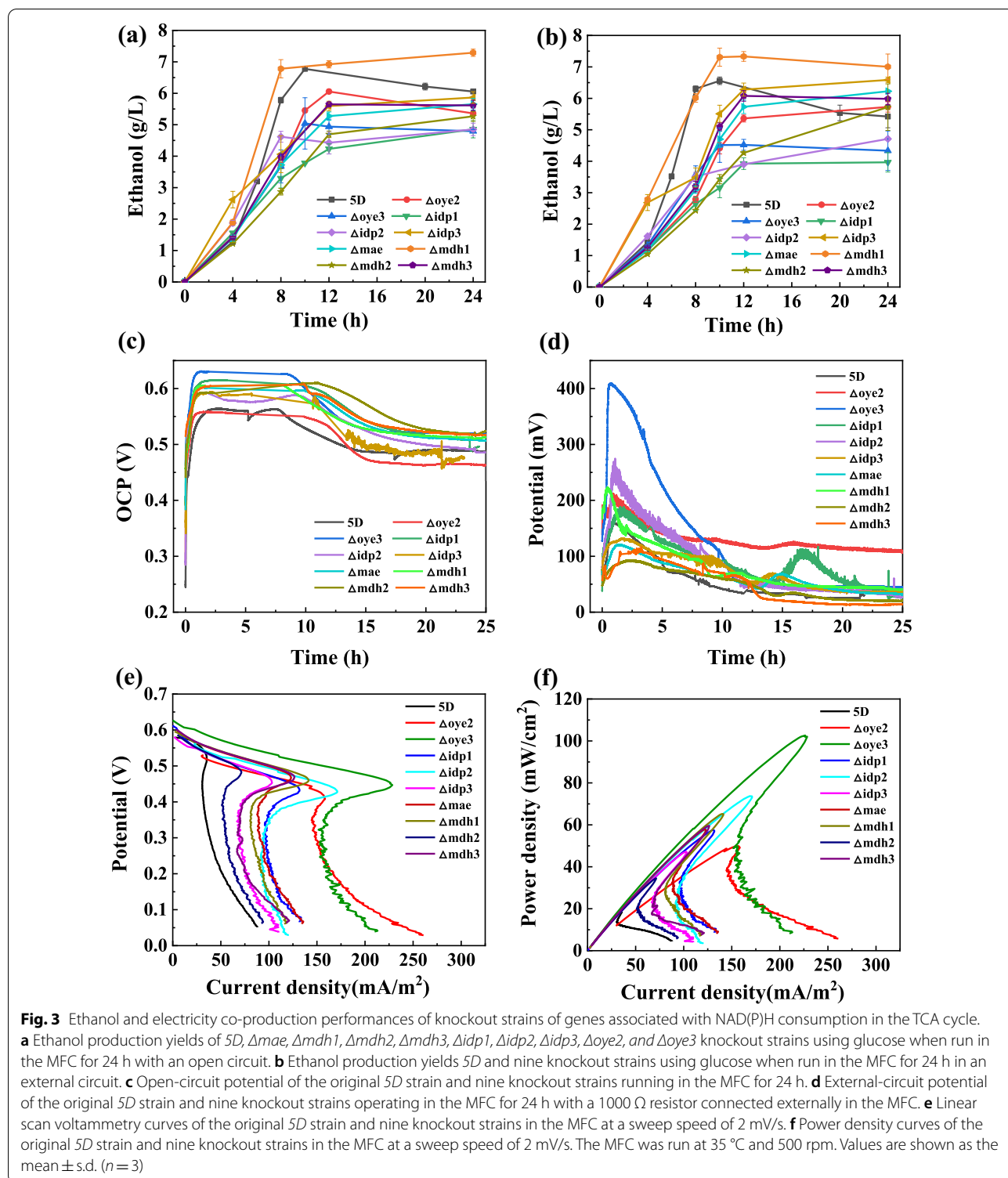
coenzymes in the TCA cycle showed a slight improvement in electrical production, indicating that the $\Delta oye3$ and $\Delta idp1$ knockout strains were able to accumulate electrons intracellularly, which led to an increase in the open-circuit and external-circuit potentials and power densities [30]. Power overshoot was also observed in knockout strains of genes associated with NAD(P)H depletion in the TCA cycle.

Performance of ethanol and electricity co-production of multi-knockout strains

The intracellular accumulation of electrons by adjusting two modules of the pyruvate metabolism and the TCA cycle improved the electricity generation performances of some of the knockout strains. Based on the above work, we chose to knock out the gene for electron accumulation in the TCA cycle based on the best performing $\Delta dld123$ knockout strain for further electron accumulation.

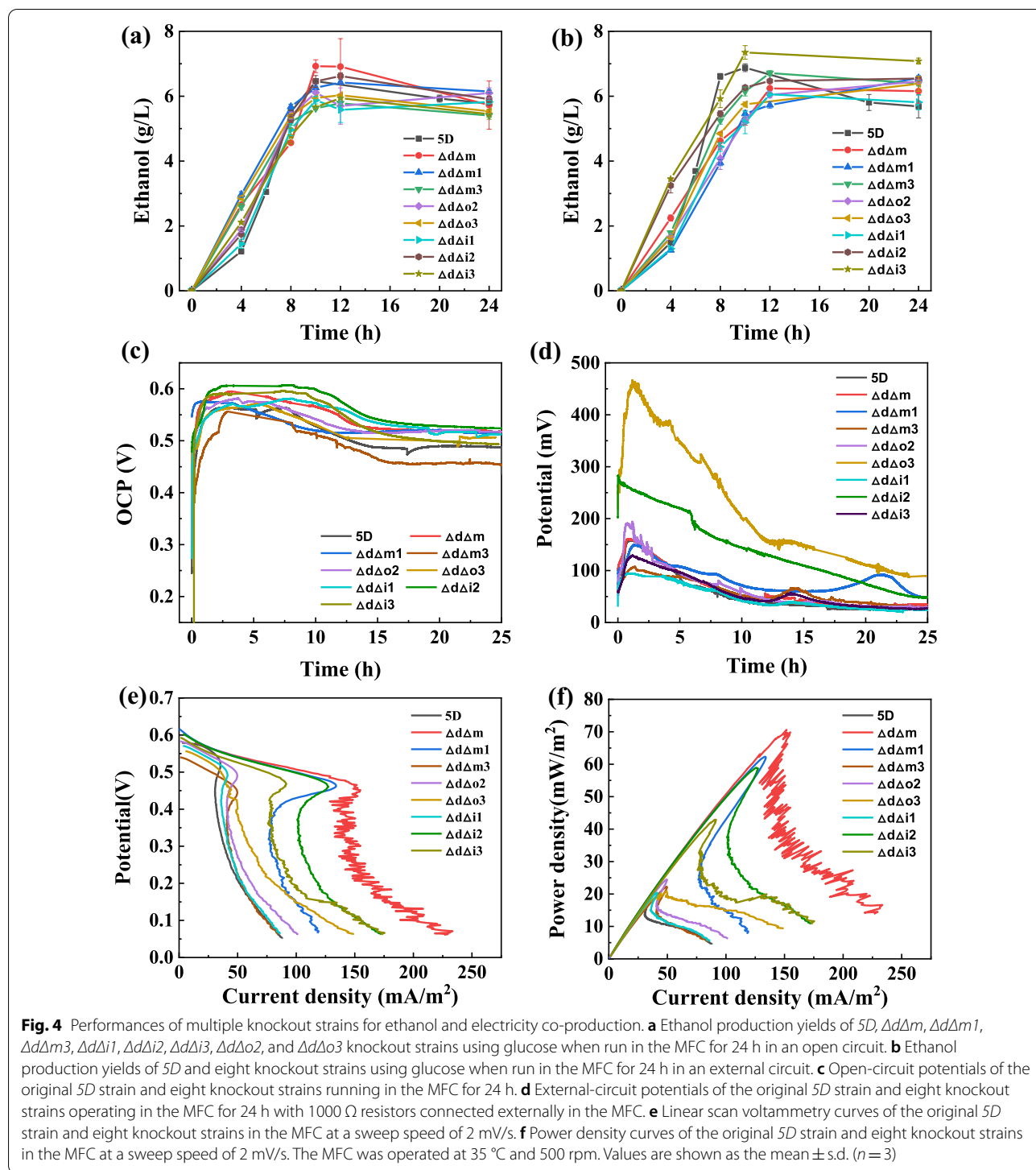
The ethanol yields of the knockout strains in the open and external circuits are shown in Fig. 4a, b, respectively. The ethanol yields of each of the multiple knockout strains were essentially the same as those of the original *SD* strain, and the glucose was consumed in the anode electrolyte at 10 h (Additional file 1: Fig. S8). Since knocking out some genes in the TCA cycle would affect the growth and metabolism of the strain, knocking out the above genes in the TCA cycle on top of the $\Delta dld123$ knockout strain resulted in the majority of knockout strains having growth amounts that were still lower than that of the original bacteria (Additional file 1: Fig. S7). The reason for the absence of significant changes in ethanol production in the multiple knockout strains may be attributed to the combined action of two modules of the pyruvate metabolism and the TCA cycle.

The open-circuit and external-circuit potentials are shown in Fig. 4c, d, respectively, for the original strain and the multiple knockout strains. The open-circuit potential of the $\Delta d\Delta i1$ knockout strain increased significantly compared to those of the other knockout strains, reaching 0.615 V, and the external-circuit potential reached a maximum of 0.283 V. The open-circuit potential increased by 34 mV, and the external-circuit potential



increased by 77% compared to those of the original strain. However, the electricity generation performance was inferior to that of the *Δdld123* with the knockdown of lactate dehydrogenase. The power densities of multiple

knockout strains *ΔdΔm*, *Δd3Δm1*, and *Δd3Δi2* were 70.6, 62.3, and 59 mW/m², respectively, which were 2–3 times higher than those of the original strain, and the rest of the strains did not differ much from the original



strain. Similarly, we observed a power overshoot in the power density curves of the multiple knockout strains. The reason for the lack of a significant effect of multiple knockout strains on improving the electricity generation performance may be that multiple knockouts have an

effect on the intracellular metabolism of the strains and the accumulated NAD(P)H acts on other metabolic pathways, leading to a re-consumption of NAD(P)H, which in turn leads to a decrease in power generation performance[38, 39].

Intracellular electron accumulation

According to our hypothesis, after the knockdown of electron-consuming genes, the intracellular electron consumption pathway was blocked and the intracellular electron accumulation increased. When the intracellular levels of total NAD (NADH+NAD⁺) and NADP (NADPH+NADP⁺) were kept constant, the increase in the intracellular releasable electrons can be presented by the NAD(P)H/NAD(P)⁺ ratio [26]. For this reason, we selected some knockout strains and cultured them in shake flasks, which were shaken at 30 °C and 200 rpm to measure NADH/NAD⁺ and NADPH/NADP⁺ ratios. The NADH/NAD⁺ ratio of the $\Delta dld123$ knockout strain was 2.8 times higher than that of the original 5D strain, and the ratio of the other knockout strains also showed varying degrees of increase (Fig. 5a). These results are consistent with our hypothesis that knockdown of lactate dehydrogenase significantly increases the number

of releasable electrons intracellularly in the form of an increased NADH content. In contrast, the number of intracellular electrons is also increased to some extent in strains knocking out some genes of the TCA cycle, but not to the same extent as in the $\Delta dld123$ knockout strain. As shown in Fig. 5(b), the intracellular NADPH/NADP⁺ values, which were 1.87 and 1.85 times higher for the $\Delta oye3$ and $\Delta idp2$ knockout strains than that of the original 5D strain, respectively. This indicates that knocking out the relevant genes from the strains in the TCA cycle mainly increases the intracellular electron accumulation in the form of an increased intracellular NADPH content. However, the increase in the intracellular NADPH content is not significant for the strains with multiple knockouts and knockout of lactate dehydrogenase. By measuring the intracellular NAD(P)H/NAD(P)⁺ ratio in the presence of electron transfer mediators in the MFCs, we observed the intracellular electron accumulation in

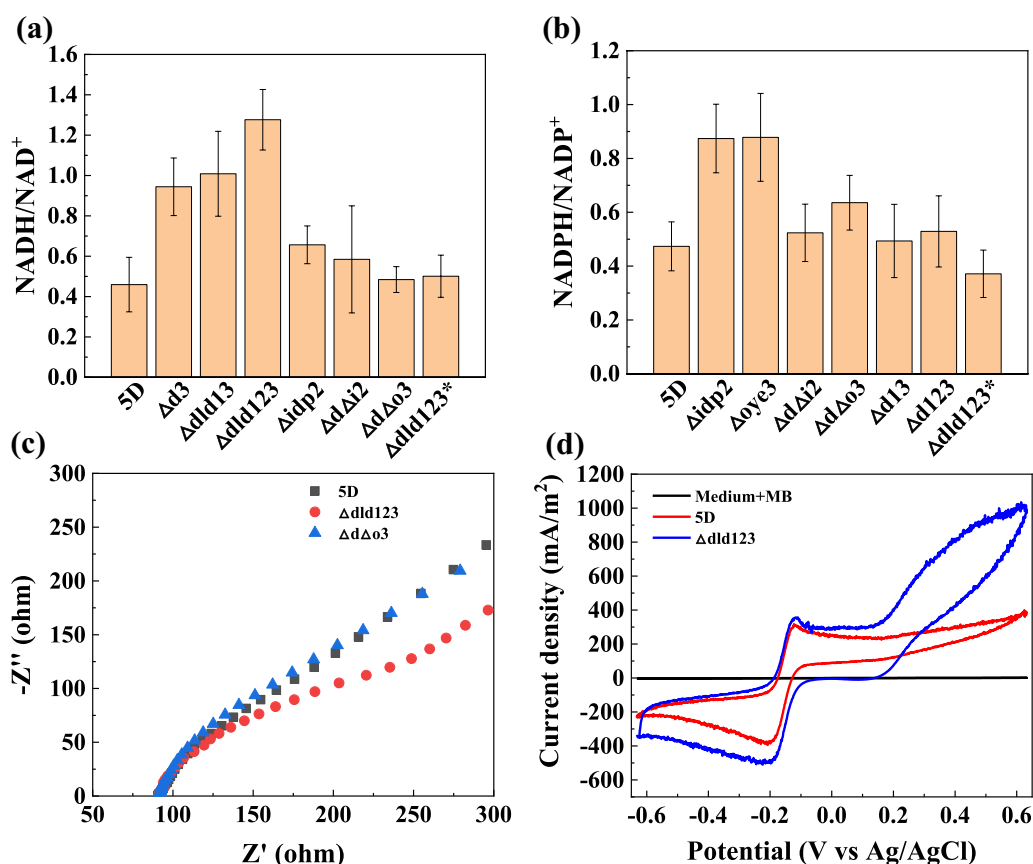


Fig. 5 Diagram of intracellular electron accumulation verification. **a** Intracellular NADH/NAD⁺ ratios of 5D and $\Delta d3$, $\Delta d13$, $\Delta d123$, $\Delta idp2$, $\Delta d\Delta i2$, $\Delta d\Delta o3$, and $\Delta dld123^*$ knockout strains cultured at 30 °C and 200 rpm in a shaker ($\Delta dld123^*$ indicates the $\Delta dld123$ knockout strain cultured in the MFC). **b** Intracellular NADPH/NADP⁺ ratio of 5D and $\Delta idp2$, $\Delta oye3$, $\Delta d\Delta i2$, $\Delta d\Delta o3$, $\Delta d13$, $\Delta d123$, and $\Delta dld123^*$ knockout strains incubated in a shaker at 30 °C and 200 rpm. **c** Electrochemical impedance spectra of 5D, $\Delta dld123$, and $\Delta d\Delta o3$ strains in a three-electrode system in the MFC. **d** Cyclic voltammograms of the blank medium and strains 5D and $\Delta dld123$ in the MFC at a sweep speed of 1 mV/s in the three-electrode system. The MFC was run at 35 °C and 500 rpm. Values are shown as the mean \pm s.d. ($n=3$)

the $\Delta dld123^*$ knockout strain was close to that of the original *5D* strain (Fig. 5a, b). This is because intracellular electrons are transferred from the cell to the electrode by extracellular electron transfer mediators, so the intracellular electron content of the $\Delta dld123$ knockout strain decreases to the same level as that of the original *5D* strain, ultimately leading to a similar NAD(P)H/NAD(P)⁺ ratio in both strains. These results suggest that the electrons accumulated in the cells of the knockout strain are transferred to the anode of the MFC. It can also be speculated that the change in ethanol and electricity co-production performance of the multiple knockout strains may be due to a decrease in total intracellular NAD(P)H content from the change in total intracellular NAD(P)H.

The internal resistance of the knockout strain on the anode was assessed by measuring the electrochemical impedance spectrum (EIS) [40] to further determine the charge-transfer internal resistance and diffusion internal resistance of the MFC [30]. Here, the original strain and the $\Delta dld123$ and $\Delta d\Delta o3$ knockout strains with higher outer circuits were selected. The electrochemical impedance spectra of all three strains are composed of a semicircle in the front and a straight line in the back. The $\Delta dld123$ strain has a distinct semicircle part, and the other two strains have less evident semicircle parts, but the diameter of the semicircle part of the $\Delta dld123$ strain is significantly smaller than that of the original strain, as shown in Fig. 5c. Since the semicircles of the EIS are not well-defined, the impedance data were fitted with the Randles equivalent circuit (Additional file 1: Fig. S9) to obtain accurate results. The charge-transfer internal resistance (R_{ct}) of the $\Delta dld123$ strain is 90 Ω , which is much smaller than that (149 Ω) of the *5D* strain, clearly indicating that the charge-transfer internal resistance of the $\Delta dld123$ strain was reduced and the EET rate was significantly increased. Therefore, knockdown of intracellular electron-consuming genes can effectively facilitate EET efficiency in *Saccharomyces cerevisiae*. By comparing with other studies, the charge-transfer internal

resistance in the microbial fuel cell mentioned in this study is much lower, showing even better performance (Table 2).

As shown in Fig. 5d, the cyclic voltammetry curves with and without *Saccharomyces cerevisiae* in the MFC, from which it can be seen that there is no current response when the anode electrolyte is medium without *Saccharomyces cerevisiae* (Additional file 1: Fig. S10), while the current response is significant when *Saccharomyces cerevisiae* is added, and $\Delta dld123$ has a larger current response than the original *5D* strain. In addition, two distinct redox peaks in the range of -0.1 V to -0.2 V are present, indicating that *Saccharomyces cerevisiae* has a distinct biocatalytic behavior. In other words, it uses glucose for oxidation reactions at the anode to provide electrons and knocking out the *dld* gene significantly increases the electrochemical activity. The internal area of the cyclic voltammogram of the $\Delta dld123$ knockout strain is significantly larger than that of the original *5D* strain, indicating a higher anodic conductance [41], i.e., a faster electron transfer rate, which is also mutually verified with the EIS images (Fig. 5c).

Calculation of energy utilization

Using *Saccharomyces cerevisiae* in the MFC for ethanol and electricity co-production, part of the energy from glucose is used for fermentation to produce ethanol without affecting the yeast growth; part of the energy can be used for electricity generation by extracting electrons generated from the NADH/NAD⁺ redox cycle using MFC technology. Thus, part of the energy originally converted to heat by the microorganisms during fermentation can be collected in the form of electricity and the utilization rate of the substrate will be improved. For this process, we calculated the energy utilization of each knockout strain in an open circuit. We used the heat of combustion values to calculate the utilization of the substrate, with an equal scaling of the MFC scale by a factor of 10. The fermentation energy utilization is calculated as

Table 2 Total internal resistance/charge-transfer internal resistance of different microbial fuel cells under the same or similar conditions

Types of microbial fuel cell anode microorganisms	Internal resistance (Ω)	Previous studies	References
Anaerobic activated sludge	82.1(R_{ct})	Yuan et al. 2011	[42]
<i>Escherichia coli</i>	134(R_{ct})	Liu et al. 2012	[30]
Mixed bacteria screened from marine surface sediments	34(R_{ct})	Du et al. 2015	[43]
Soil microbial	183	Li et al. 2016	[44]
The effluent from existing MFCs during operation	187	Kim et al. 2021	[32]
<i>Saccharomyces cerevisiae</i>	90(R_{ct})	–	This Study

$$\eta_1 = n_{\text{eth}} * \Delta H_{\text{eth}} / n_{\text{glu}} * \Delta H_{\text{glu}}, \quad (1)$$

where n_{eth} and n_{glu} are the amounts of ethanol and glucose in the fermentation process, respectively, and ΔH_{eth} and ΔH_{glu} are the heats of combustion of ethanol and glucose, respectively.

The energy utilization during electricity generation is calculated with the following assumptions: the operation is carried out for 24 h at maximum power density, the volume scale is enlarged 10 times to 1 L, and the electrode size is enlarged 10 times in equal proportion. The energy utilization of power generation is defined as:

$$\eta_2 = P * S * t / n_{\text{glu}} * \Delta H_{\text{glu}}, \quad (2)$$

where P is the MFC power density, S is the electrode area, and t is the MFC operation time.

As shown in Table 3, the substrate energy utilization of some knockout strains is improved to some extent, with the $\Delta dld123$ knockout strain increasing by 17.3% compared to that of the original strain. This indicates that the utilization of the substrate glucose can be improved by modifying *Saccharomyces cerevisiae* and applying it to the MFC.

Discussion

The low power of MFCs is currently the main constraint for MFC applications [45]. The electroactive microorganisms in MFCs are mainly electroactive bacteria, such as *Geobacter sulfurreducens* [46], *Shewanella oneidensis MR-1* [47], archaea [48], and eukaryotic microorganisms [21]. Current research on electroactive microorganisms also includes the modification of new genetically engineered microorganisms, such as *E. coli* [49] and *Saccharomyces cerevisiae* [50], to provide the MFC with more efficient electron transfer and increase the EET. There are currently two main strategies to improve MFC performance. One is to increase the EET rate, for example, by improving the electrode materials [51–53] or microbial co-culture to secrete extracellular polymers (e.g., riboflavin) [9, 54], and the other is to increase intracellular electron accumulation to increase the electron supply. In microbial cells, increasing the supply of electrons can be achieved by various methods, including introducing exogenous genes that enhance intracellular NADH regeneration [36, 55], targeting metabolic fluxes for NAD⁺ biosynthesis using modular engineering [56, 57], and knocking down intracellular reductive metabolic pathways [26]. Knocking out of lactate synthesis pathway genes [26] and central metabolism genes [38] in *E. coli* increases the

Table 3 Summary of energy utilization values of knockout strains

Strains	Fermentation energy utilization (%)	Electricity generation energy utilization (%)	Total energy utilization (%)
5D	61.6	0.5	62.1
$\Delta dld1$	57.9	1.3	59.2
$\Delta dld2$	54.4	1.5	55.8
$\Delta dld3$	52.0	1.2	53.2
$\Delta dld12$	67.2	1.4	68.6
$\Delta dld13$	52.8	1.1	53.8
$\Delta dld23$	56.7	1.0	57.7
$\Delta dld123$	71.8	7.6	79.4
$\Delta oye2$	57.8	1.5	59.2
$\Delta oye3$	48.1	2.9	51.0
$\Delta idp1$	46.3	1.6	47.9
$\Delta idp2$	46.6	2.1	48.7
$\Delta idp3$	60.9	1.7	62.6
Δmae	53.9	1.7	55.6
$\Delta mdh1$	69.5	2.0	71.5
$\Delta mdh2$	50.2	1.0	51.3
$\Delta mdh3$	53.9	1.7	55.5
$\Delta d\Delta o2$	61.8	0.7	62.5
$\Delta d\Delta o3$	61.5	0.6	62.1
$\Delta d\Delta i1$	58.3	0.6	58.8
$\Delta d\Delta i2$	63.1	1.7	64.9
$\Delta d\Delta i3$	70.1	1.3	71.4
$\Delta d\Delta m$	66.0	1.8	67.9
$\Delta d\Delta m1$	61.2	2.0	63.2
$\Delta d\Delta m3$	63.1	0.0	63.2

intracellularly releasable electrons, which are subsequently transferred to the anode via an electron transfer medium, improving the MFC electrical production performance.

Saccharomyces cerevisiae is a microorganism suitable for industrial production, and its fermentation of glucose for ethanol production is accompanied by the oxidation of large amounts of NADH to NAD⁺ (electron consumption pathway) [58, 59]. This property of *Saccharomyces cerevisiae* makes it an ideal anode microbial catalyst in microbial fuel cells. For the improvement of yeast microbial fuel cell performance, Manisha Verma et al. summarized that the current methods are addition of artificial mediators, anode surface modification, yeast cell immobilization, yeast surface display method, genetically modified yeast cell, etc. [60].

Here, we enhance the performance of MFC by modulating in vivo metabolism in *Saccharomyces cerevisiae*. Knockdown of genes involved in the depletion of NAD(P)H allows intracellular accumulation of reduced coenzymes (i.e., electrons).

Conclusion

In this study, it was found that the knockdown of intracellular electron-consuming genes allowed the accumulation of excess electrons in cells, and the elevated intracellular electron pool positively influenced the electrical production performance of the MFC. Furthermore, by knocking out the intracellular metabolic pathway, the yield of ethanol could be increased, and co-production of ethanol and electricity could be achieved. Thus, the MFC improved the utilization of the substrate. The highest ethanol yield of the knockout strain reached 7.71 g/L, and the highest power density in the MFC reached 240 mW/m², which was 12 times higher than that of the control bacteria. In addition, the energy utilization was 17.3% higher than that of the control bacteria. Since there are many electron-consuming and electron-generating pathways in *Saccharomyces cerevisiae*, our work explored the reduction of electron consumption. We will subsequently consider enhancing the electron-generating pathways to enhance intracellular electron accumulation and further improve the electricity production performance. In addition, enhancements in terms of ethanol production, such as improving carbon utilization through CO₂ reuse [61], can be considered. This work provides a reference for subsequent in vivo metabolic engineering of microorganisms to regulate intracellular electron accumulation for bioelectricity production in MFCs.

Methods

Strain construction

The *Saccharomyces cerevisiae* used in the experiments had the conservation number CEN.PK 117-5D. The lactate dehydrogenase genes *dld1*, *dld2*, and *dld3* in the pyruvate metabolism were knocked out using CRISPR/Cas9. The same approach was used to knock out some of the genes related to the consumption of reduced coenzymes in the citric acid cycle, including *mae*, *mdh1*, *mdh2*, *mdh3*, *idp1*, *idp2*, *idp3*, *oye2*, and *oye3*. Additional file 1: Table S1 and Sect. 1.1 of the additional file information list the specific primers and methods of operation.

Preparation of cathode and anode chambers

For the cathode electrolyte, 0.5 g of potassium ferricyanide (Macklin biochemical Co., Ltd, China, Shanghai) was dissolved in 100 ml of phosphate buffer solution (PBS) with a pH of 6.5 to obtain a 5 g/L solution. The anode electrolyte contained basal medium (7.5 g/L NH₄SO₄ (Macklin biochemical Co., Ltd, China, Shanghai), 14.4 g/L KH₂PO₄ (Aladdin Biochemical Technology Co., Ltd, China, Shanghai), 0.5 g/L MgSO₄·7H₂O (Sinopharm Chemical Reagent Co., Ltd, China, Beijing), 0.1% vitamin solution, and 0.1% trace metal solution [62]). The

anode electrolyte was adjusted to a pH of 6.5 with KOH and autoclaved at 116 °C for 25 min.

Construction of microbial fuel cells

The microbial fuel cell device was a typical H-type microbial fuel cell, consisting of two glass bottles with volumes of 100 ml. The cathode and anode chambers were separated with Nafion 117 membranes (DuPont, USA, State of Delaware). Carbon cloth was used as the electrodes with anode electrode sizes of 2.5 × 3 cm and cathode electrode sizes of 3 × 3 cm. Carbon cloth electrodes and proton exchange membranes were treated (Additional file 1: Sect. 1.2), and the microbial fuel cell device was assembled in an ultraclean bench. Since oxygen is beneficial for the pre-growth of microorganisms, the anode electrolyte was not treated with N₂ venting. A 1 kΩ resistor was connected externally for all the external-circuit potential measurements.

Saccharomyces cerevisiae strains were inoculated into yeast extract peptone dextrose (YPD) medium (20 g/L glucose (Sinopharm Chemical Reagent Co., Ltd, China, Beijing), 20 g/L peptone (Oxoid, UK), and 10 g/L yeast extract (Oxoid, UK)) and incubated at 30 °C and 200 rpm. Yeast cells were inoculated into the anode chamber after centrifugation and washing with an initial optical density (OD) of approximately 1.5. The microbial fuel cell device was placed on a magnetic hot plate at 35 °C with continuous agitation of the anode electrolyte at 500 rpm/min to ensure the growth of the anode microorganisms and the contact of the microorganisms with the electrodes. The sampling port was disinfected by spraying 75% ethanol before sampling, and samples were taken with sterile syringes.

Analysis of products and electrochemistry

The biomass of the electricity generation process was determined by measuring the absorbance values of the samples at 600 nm using a UV spectrophotometer (OnLab, China, Shanghai). An LC20-AT high-performance liquid chromatograph (Shimadzu, Japan) was used to detect the concentration of glucose and ethanol in the anode electrolyte. A BIO-Rad 87H column was used with 5 mM sulfuric acid as the mobile phase, a column temperature of 65 °C, a flow rate of 0.6 ml/min, an injection volume of 10 μL, and a detector with an oscillometric detector. Intracellular NAD(P)⁺ and NAD(P)H were analyzed using NADH/ NAD⁺ and NADPH/ NADP⁺ quantification kit (Suzhou Comin Biotechnology Co., Ltd., USA). The open-circuit potential and external-circuit potential of the MFC were measured using a potentiostat (CHI660E, Chenhua Co., Ltd., China, Shanghai). The polarization curves

were obtained using linear scanning voltammetry with a sweep rate of 2 mV/s. Cyclic voltammetry and electrochemical impedance spectroscopy (EIS) were conducted using a three-electrode system with Ag/AgCl as the reference electrode and a cyclic voltammetry scan rate of 1 mV/s. EIS were conducted over a frequency range of 0.01 Hz to 100 kHz at open circuit potential, with a perturbation signal of 10 mV. Nyquist plots were simulated as an equivalent circuit (Additional file 1: Fig. S9) using a fitting program (ZsimpWin 3.10).

Abbreviations

MFCs: Microbial fuel cells; DET: Direct electron transfer; EET: Extracellular electron transfer; OCP: Open-circuit potential; MB: Methylene blue; TCA cycle: Tricarboxylic acid cycle; EIS: Electrochemical impedance spectroscopy.

Supplementary Information

The online version contains supplementary material available at <https://doi.org/10.1186/s13068-022-02180-4>.

Additional file 1: Figure. S1. Growth curves of lactate dehydrogenase knockout strains in MFC run in (a) open circuit for 24 h; (b) external circuit for 24 h. **Figure. S2.** Glucose consumption curve of lactate dehydrogenase knockout strains in MFC run in (a) open circuit for 24 h; (b) external circuit for 24 h. **Figure. S3.** Open circuit voltage of lactate dehydrogenase knockout strains running in MFC for 24 h. **Figure. S4.** (a) Linear scanning voltammetry curves of the lactate dehydrogenase knockout strain in MFC at a sweep speed of 2 mV/s; (b) power density curves of the lactate dehydrogenase knockout strain in MFC at a sweep speed of 2 mV/s. **Figure. S5.** Growth curves of knockout strains associated with NAD(P)H depletion in the TCA cycle in MFC run in (a) open circuit for 24 h; (b) external circuit for 24 h. **Figure. S6.** Glucose consumption curve of knockout strains associated with NAD(P)H depletion in the TCA cycle in MFC run in (a) open circuit for 24 h; (b) external circuit for 24 h. **Figure. S7.** Growth curves of multi-knockout strains in MFC run in (a) open circuit for 24 h; (b) external circuit for 24 h. **Figure. S8.** Glucose consumption curve of multi-knockout strains in MFC run in (a) open circuit for 24 h; (b) external circuit for 24 h. **Figure. S9.** The schematic of an equivalent circuit model (R(Q|RW)). **Figure. S10.** Cyclic voltammetry curve of the blank control at a sweep speed of 1 mV/s. **Table S1.** Relevant primers for constructing knockout plasmids (genes *dld1*, *dld2*, *dld3*, *mae*, *mdh1*, *mdh2*, *mdh3*, *oye2*, *oye3*, *idp1*, *idp2*, *idp3*). **Table S2.** Construction of knockout plasmids for donor (genes *dld1*, *dld2*, *dld3*, *mae*, *mdh1*, *mdh2*, *mdh3*, *oye2*, *oye3*, *idp1*, *idp2*, *idp3*). **Table S3.** Name of strains used in this study. **Table S4.** Summary of the highest ethanol yields for each knockout strain.

Acknowledgements

The authors thank the National Natural Science Foundation of China (U21B2098), National Natural Science Foundation of China (21811530003), National Key Research and Development Program of China (2018YFB1501704).

Author contributions

RX, SW, KW and TWT designed the research; RX, SW and KW performed the experiments; RX, KW analyzed the data; RX, SW, KW, ZW, MW, BQC and TWT wrote the paper with contribution from all authors. All authors read and approved the final manuscript.

Funding

This work is supported by National Natural Science Foundation of China (U21B2098), National Natural Science Foundation of China (21811530003), National Key Research and Development Program of China (2018YFB1501704).

Availability of data and materials

All data generated or analyzed during this study are included in this published article and its additional files.

Declarations

Ethics approval and consent to participate

Not applicable.

Consent for publication

Not applicable.

Competing interests

The authors declare that they have no competing interests.

Received: 11 April 2022 Accepted: 2 August 2022

Published online: 17 August 2022

References

- Liu Z, Wang K, Chen Y, Tan T, Nielsen J. Third-generation biorefineries as the means to produce fuels and chemicals from CO₂. *Nat Catal*. 2020;3(3):274–88.
- Chu S, Majumdar A. Opportunities and challenges for a sustainable energy future. *Nature*. 2012;488(7411):294–303.
- Mohd Azhar SH, Abdulla R, Jambo SA, Marbawi H, Gansau JA, Mohd Faik AA, Rodrigues KF. Yeasts in sustainable bioethanol production: a review. *Biochem Biophys Rep*. 2017;10:52–61.
- Nandy SK, Srivastava RK. A review on sustainable yeast biotechnological processes and applications. *Micribiol Res*. 2018;207:83–90.
- Wills C. Regulation of sugar and ethanol metabolism in *Saccharomyces cerevisiae*. *Crit Rev Biochem Mol*. 1990;25(4):245–80.
- Gunawardena A, Fernando S, To F. Performance of a yeast-mediated biological fuel cell. *Int J Mol Sci*. 2008;9(10):1893–907.
- Freguia S, Rabaey K, Yuan Z, Keller J. Syntrophic processes drive the conversion of glucose in microbial fuel cell anodes. *Environ Sci Technol*. 2008;42(21):7937–43.
- Chaudhuri SK, Lovley DR. Electricity generation by direct oxidation of glucose in mediatorless microbial fuel cells. *Nat Biotechnol*. 2003;21(10):1229–32.
- Yang Y, Wu Y, Hu Y, Cao Y, Poh CL, Cao B, Song H. Engineering electrode-attached microbial consortia for high-performance xylose-fed microbial fuel cell. *ACS Catal*. 2015;5(11):6937–45.
- Hassan SHA, Kim YS, Oh S-E. Power generation from cellulose using mixed and pure cultures of cellulose-degrading bacteria in a microbial fuel cell. *Enzyme Microb Tech*. 2012;51(5):269–73.
- Cui Y, Rashid N, Hu N, Rehman MSU, Han J-I. Electricity generation and microalgae cultivation in microbial fuel cell using microalgae-enriched anode and bio-cathode. *Energy Convers Manag*. 2014;79:674–80.
- Karthikeyan R, Selvam A, Cheng KY, Wong JW-C. Influence of ionic conductivity in bioelectricity production from saline domestic sewage sludge in microbial fuel cells. *Bioresour Technol*. 2016;200:845–52.
- Intasian P, Prakinee K, Phintha A, Trisrivirat D, Weeranoppanant N, Wongnate T, Chaiyen P. Enzymes, in vivo biocatalysis, and metabolic engineering for enabling a circular economy and sustainability. *Chem Rev*. 2021;121(17):10367–451.
- García-Mayagoitia S, Fernández-Luqueño F, Morales-Acosta D, Carrillo-Rodríguez JC, García-Lobato MA, de la Torre-Saenz L, Alonso-Lemus IL, Rodríguez-Varela FJ. Energy generation from pharmaceutical residual water in microbial fuel cells using ordered mesoporous carbon and *Bacillus subtilis* as bioanode. *ACS Sustain Chem Eng*. 2019;7(14):12179–87.
- Zhong C, Zhang B, Kong L, Xue A, Ni J. Electricity generation from molasses wastewater by an anaerobic baffled stacking microbial fuel cell. *J Chem Technol Biot*. 2011;86(3):406–13.
- He L, Du P, Chen Y, Lu H, Cheng X, Chang B, Wang Z. Advances in microbial fuel cells for wastewater treatment. *Renew Sust Energy Rev*. 2017;71:388–403.

17. Wang Z, Lee T, Lim B, Choi C, Park J. Microbial community structures differentiated in a single-chamber air-cathode microbial fuel cell fueled with rice straw hydrolysate. *Biotechnol Biofuels*. 2014;7(1):9.
18. Verma M, Verma MK, Singh V, Singh J, Singh V, Mishra V. Advancements in applicability of microbial fuel cell for energy recovery from human waste. *Bioresour Technol Rep*. 2022;17: 100978.
19. Abou Jarboua T, Davison M, Karamanev D. Cost analysis of a 1 MW biogenerator, a bioelectrochemical technology for energy storage. *J Energy Storage*. 2019;21:328–36.
20. Ulusoy I, Dimoglo A. Electricity generation in microbial fuel cell systems with *Thiobacillus ferrooxidans* as the cathode microorganism. *Int J Hydrogen Energy*. 2018;43(2):1171–8.
21. Logan BE, Rossi R, Ragab A, Saikaly PE. Electroactive microorganisms in bioelectrochemical systems. *Nat Rev Microbiol*. 2019;17(5):307–19.
22. Guo Y, Wang G, Zhang H, Wen H, Li W. Effects of biofilm transfer and electron mediators transfer on *Klebsiella quasipneumoniae* sp 203 electricity generation performance in MFCs. *Biotechnol Biofuels*. 2020;13(1):162.
23. Ramanavicius S, Ramanavicius A. Charge transfer and biocompatibility aspects in conducting polymer-based enzymatic biosensors and biofuel cells. *Nanomaterials*. 2021;11(2):371.
24. Ramanavicius S, Ramanavicius A. Conducting polymers in the design of biosensors and biofuel cells. *Polymers*. 2020;13(1):49.
25. Ramanavicius S, Ramanavicius A. Progress and Insights in the application of MXenes as New 2D nano-materials suitable for biosensors and biofuel cell design. *Int J Mol Sci*. 2020;21(23):9224.
26. Yong Y-C, Yu Y-Y, Yang Y, Li CM, Jiang R, Wang X, Wang J-Y, Song H. Increasing intracellular releasable electrons dramatically enhances bioelectricity output in microbial fuel cells. *Electrochem Commun*. 2012;19:13–6.
27. Fadzli FS, Bhawani SA, Adam Mohammad RE. Microbial fuel cell: recent developments in organic substrate use and bacterial electrode interaction. *J Chem*. 2021;2021:4570388.
28. Chae K-J, Choi M-J, Lee J-W, Kim K-Y, Kim IS. Effect of different substrates on the performance, bacterial diversity, and bacterial viability in microbial fuel cells. *Bioresour Technol*. 2009;100(14):3518–25.
29. Jadhav GS, Ghangrekar MM. Performance of microbial fuel cell subjected to variation in pH, temperature, external load and substrate concentration. *Bioresour Technol*. 2009;100(2):717–23.
30. Liu J, Yong Y-C, Song H, Li CM. Activation enhancement of citric acid cycle to promote bioelectrocatalytic activity of arcA Knockout *Escherichia coli* toward high-performance microbial fuel cell. *ACS Catal*. 2012;2(8):1749–52.
31. Zhang P-Y, Liu Z-L. Experimental study of the microbial fuel cell internal resistance. *J Power Sources*. 2010;195(24):8013–8.
32. Kim B, Chang IS, Dinsdale RM, Guwy AJ. Accurate measurement of internal resistance in microbial fuel cells by improved scanning electrochemical impedance spectroscopy. *Electrochim Acta*. 2021;366: 137388.
33. Kim B, An J, Chang IS. Elimination of power overshoot at bioanode through assistance current in microbial fuel cells. *Chemosuschem*. 2017;10(3):612–7.
34. Ieropoulos I, Winfield J, Greenman J. Effects of flow-rate, inoculum and time on the internal resistance of microbial fuel cells. *Bioresour Technol*. 2010;101(10):3520–5.
35. Hong Y, Call DF, Werner CM, Logan BE. Adaptation to high current using low external resistances eliminates power overshoot in microbial fuel cells. *Biosens Bioelectron*. 2011;28(1):71–6.
36. Li F, Li Y, Sun L, Chen X, An X, Yin C, Cao Y, Wu H, Song H. Modular engineering intracellular NADH regeneration boosts extracellular electron transfer of *Shewanella oneidensis* MR-1. *ACS Synth Biol*. 2018;7(3):885–95.
37. Ryan DG, Frezza C, O'Neill LAJ. TCA cycle signalling and the evolution of eukaryotes. *Curr Opin Biotech*. 2021;68:72–88.
38. Ojima Y, Kawaguchi T, Fukui S, Kikuchi R, Terao K, Koma D, Ohmoto T, Azuma M. Promoted performance of microbial fuel cells using *Escherichia coli* cells with multiple-knockout of central metabolism genes. *Bioprocess Biosyst Eng*. 2020;43(2):323–32.
39. Moriyama S, Nishio K, Mizushima T. Structure of glyoxysomal malate dehydrogenase (MDH3) from *Saccharomyces cerevisiae*. *Acta Crystallogr Sect F*. 2018;74(10):617–24.
40. Borole AP, Aaron D, Hamilton CY, Tsouris C. Understanding long-term changes in microbial fuel cell performance using electrochemical impedance spectroscopy. *Environ Sci Technol*. 2010;44(7):2740–5.
41. Tran VH, Kim E, Jung SP. Anode biofilm maturation time, stable cell performance time, and time-course electrochemistry in a single-chamber microbial fuel cell with a brush-anode. *J Ind Eng Chem*. 2022;106(269):278.
42. Yuan Y, Zhao B, Zhou S, Zhong S, Zhuang L. Electrocatalytic activity of anodic biofilm responses to pH changes in microbial fuel cells. *Bioresour Technol*. 2011;102(13):6887–91.
43. Du Y, Feng Y, Teng Q, Li H. Effect of inorganic salt in the culture on microbial fuel cells performance. *Int J Electrochemicalence*. 2015;10(2):1316–25.
44. Li X, Wang X, Zhao Q, Wan L, Li Y, Zhou Q. Carbon fiber enhanced bioelectricity generation in soil microbial fuel cells. *Biosens Bioelectron*. 2016;85:135–41.
45. Li M, Zhou M, Tian X, Tan C, McDaniel CT, Hassett DJ, Gu T. Microbial fuel cell (MFC) power performance improvement through enhanced microbial electrogenicity. *Biotechnol Adv*. 2018;36(4):1316–27.
46. Stockl M, Teubner NC, Holtmann D, Mangold KM, Sand W. Extracellular polymeric substances from *Geobacter sulfurreducens* biofilms in microbial fuel cells. *ACS Appl Mater Interfaces*. 2019;11(9):8961–8.
47. Li F, Li Y, Sun L, Li X, Yin C, An X, Chen X, Tian Y, Song H. Engineering *Shewanella oneidensis* enables xylose-fed microbial fuel cell. *Biotechnol Biofuels*. 2017;10:196.
48. Yu L, He D, Zhang E, He Q, Li J, Jason Ren Z, Zhou S. Electricity from anaerobic methane oxidation by a single methanogenic archaeon *Methanosarcina barkeri*. *Chem Eng J*. 2021;405: 126691.
49. Wang VB, Sivakumar K, Yang L, Zhang Q, Kjelleberg S, Loo SC, Cao B. Metabolite-enabled mutualistic interaction between *Shewanella oneidensis* and *Escherichia coli* in a co-culture using an electrode as electron acceptor. *Sci Rep*. 2015;5:11222.
50. Lin T, Bai X, Hu Y, Li B, Yuan YJ, Song H, Yang Y, Wang J. Synthetic *Saccharomyces cerevisiae*-*Shewanella oneidensis* consortium enables glucose-fed high-performance microbial fuel cell. *AIChE J*. 2016;63(6):1830–8.
51. Gnanakumar G, Kirubakaran CJ, Udhayakumar S, Ramachandran K, Karthikeyan C, Renganathan R, Nahm KS. Synthesis, structural, and morphological characterizations of reduced graphene oxide-supported polypyrrole anode catalysts for improved microbial fuel cell performances. *ACS Sustain Chem Eng*. 2014;2(10):2283–90.
52. Lee M-H, Thomas JL, Chen W-J, Li M-H, Shih C-P, Lin H-Y. Fabrication of bacteria-imprinted polymer coated electrodes for microbial fuel cells. *ACS Sustain Chem Eng*. 2015;3(6):1190–6.
53. Yamashita T, Yokoyama H. Molybdenum anode: a novel electrode for enhanced power generation in microbial fuel cells, identified via extensive screening of metal electrodes. *Biotechnol Biofuels*. 2018;11(1):39.
54. Bai X, Lin T, Liang N, Li B-Z, Song H, Yuan Y-J. Engineering synthetic microbial consortium for efficient conversion of lactate from glucose and xylose to generate electricity. *Biochem Eng J*. 2021;172:108052.
55. Han S, Gao X-y, Ying H-j, Zhou CC. NADH gene manipulation for advancing bioelectricity in *Clostridium ljungdahlii* microbial fuel cells. *Green Chem*. 2016;18(8):2473–8.
56. Li F, Li YX, Cao YX, Wang L, Liu CG, Shi L, Song H. Modular engineering to increase intracellular NAD (H⁺) promotes rate of extracellular electron transfer of *Shewanella oneidensis*. *Nat Commun*. 2018;9(1):3637.
57. Qin N, Li L, Ji X, Li X, Zhang Y, Larsson C, Chen Y, Nielsen J, Liu Z. Rewiring central carbon metabolism ensures increased provision of Acetyl-CoA and NADPH required for 3-OH-Propionic acid production. *ACS Synth Biol*. 2020;9(12):3236–44.
58. Adachi E, Torigoe M, Sugiyama M, Nikawa J-I, Shimizu K. Modification of metabolic pathways of *Saccharomyces cerevisiae* by the expression of lactate dehydrogenase and deletion of pyruvate decarboxylase genes for the lactic acid fermentation at low pH value. *J Ferment Bioeng*. 1998;86(3):284–9.
59. Xia P-F, Zhang G-C, Walker B, Seo S-O, Kwak S, Liu J-J, Kim H, Ort DR, Wang S-G, Jin Y-S. Recycling carbon dioxide during xylose fermentation by engineered *Saccharomyces cerevisiae*. *ACS Synth Biol*. 2017;6(2):276–83.
60. Verma M, Mishra V. Recent trends in upgrading the performance of yeast as electrode biocatalyst in microbial fuel cells. *Chemosphere*. 2021;284: 131383.
61. Kazemi M, Biria D, Rismani-Yazdi H. Modelling bio-electrosynthesis in a reverse microbial fuel cell to produce acetate from CO₂ and H₂O. *Phys Chem Chem Phys*. 2015;17(19):12561–74.
62. Taherzadeh MJ, Lidén G, Gustafsson L, Niklasson C. The effects of pantothenate deficiency and acetate addition on anaerobic batch fermentation of glucose by *Saccharomyces cerevisiae*. *Appl Microbiol Biot*. 1996;46(2):176–82.

Publisher's Note

Springer Nature remains neutral with regard to jurisdictional claims in published maps and institutional affiliations.